Contribution from the Department of Chemistry,
University of Georgia, Athens, Georgia 30602

Topological Aspects of the Chemical Bonding in Superconducting Transition-Metal Borides, Silicides, and Alloys

R. B. King

Received August 11, 1989

The porous delocalization apparently required for superconductivity in solid-state materials has the following essential features: (1) edge-localized chemical bonding topology of the conducting skeleton leading to a porous rather than dense volume in which electron transport can take place; (2) holes in the valence band that can be delocalized throughout the porous conducting skeleton, thereby providing a mechanism for electron transport. Ternary transition-metal boride superconductors exhibiting such porous delocalization include $LnRh_4B_4$ (Ln = lanthanide) constructed from rhodium tetrahedra, $Ba_{0.67}Pt_3B_2$ constructed from platinum triangles, $LnRuB_2$ constructed from ruthenium chains, and $LnOs_3B_2$ constructed from osmium trigonal prisms. Ternary transition-metal silicide superconductors are of two general types: (1) superconducting silicides with structures derived from the $BaAl_4$ structure containing delocalized tetragonal pyramidal cavities with supplemental edge-localized bonding as exemplified by $Lu_2Fe_3Si_5$, $La_2Rh_3Si_5$, and $LaIr_2Si_2$; (2) superconducting silicides having a transition-metal–silicon conducting skeleton exhibiting edge-localized chemical bonding as exemplified by $Sc_5Ir_4Si_{10}$, $LaRhSi_2$, LaPtSi, ThIrSi, and $LaRu_3Si_2$. The conducting skeleton for the A-15 alloy superconductors M_3E (M = V, Nb, Ta; E = Si, Ge, Sn) consists of infinite straight M_∞ chains in each of the three orthogonal directions with edge-localized chemical bonding topology in these chains leading to an $M_6E_2^{2-}$ closed-shell electronic configuration. Topological methods can also be used to rationalize empirical rules for the relationship of the critical superconducting temperature in transition-metal alloys to the average number of valence electrons per atom (Z_{av}) where maxima are observed at $Z_{av} = 4.8$ and $Z_{av} = 7$ and to a lesser extent at $Z_{av} = 3.3$.

Introduction

Application of graph-theory-derived methods[1-5] to the study of the chemical bonding topology in ternary molybdenum chalcogenides MMo_6S_8 (Chevrel phases)[6] and ternary lanthanide rhodium borides[7] suggests a connection between relatively high superconducting critical temperatures (e.g. $T_c > 4$ K) and a conducting skeleton having an edge-localized chemical bonding topology with holes in the valence band conveniently designated as porous delocalization. Subsequent work showed that these ideas could be extended to the high-T_c copper oxide superconductors to provide a simple rationalization why the T_c's of the copper oxide superconductors are much higher than those of any of the known metal cluster superconductors.[8,9]

This paper uses a similar approach to study the chemical bonding topology of diverse solid-state transition-metal structures exhibiting superconductivity, including transition metal borides, silicides, and alloys. An important conclusion from this work is the observation that the conducting skeletons of essentially all such superconductors exhibit the edge-localized chemical bonding topology with holes in the valence band that is characteristic of porous delocalization, thereby supporting further the connection between superconductivity and porous delocalization.

Background

The two extreme types of skeletal chemical bonding in metal clusters may be called edge-localized and globally delocalized.[1-5] An edge-localized skeleton has two-electron–two-center metal–metal bonds along each edge of the skeleton and is favored when the numbers of metal internal orbitals match the vertex degrees (i.e., the number of edges meeting at the (metal) vertex in question). A globally delocalized skeleton is constructed from metal polyhedra with multicenter core bonds in the center of the polyhedra and is favored when the numbers of internal orbitals do not match the vertex degrees. Since metal cluster vertices normally use three internal orbitals for skeletal chemical bonding, metal cluster structures constructed from polyhedra having all vertices of degree 3 such as the tetrahedron or trigonal prism normally exhibit edge-localized bonding. However, metal cluster structures based on regular octahedra, which have all vertices of degree 4, normally exhibit globally delocalized bonding with a six-center core bond in the center of the octahedron. However, early-transition-metal vertices can use four rather than three internal orbitals, leading to edge-localized octahedra rather than globally delocalized octahedra. Such an abnormal situation is found in the Mo_6 octahedra, which are the building blocks for the Chevrel phase superconductors MMo_6S_8.[6] Evidence for the relevance of edge-localized skeletal bonding to superconductivity is provided by the observation that the only superconductors constructed from metal octahedra are the Chevrel phases, which have exceptional edge-localized metal octahedra rather than the normal globally delocalized metal octahedra.

The superconducting ternary transition-metal boride and silicide superconducting structures are summarized in Tables I and II. Their conducting skeletons consist of their transition-metal–boron or metal–silicon subnetworks with the more electropositive lanthanide or alkaline-earth metal furnishing additional electrons to this skeleton. The exclusion of the more electropositive lanthanides from the conducting skeleton accounts for the retention of some superconductivity, albeit with lower T_c's, in some cases when magnetic lanthanides are introduced into the ternary boride or silicide structure. The T_c values given in Tables I and II are for compounds containing nonmagnetic electropositive metals such as the alkaline earths, scandium, lanthanum, lutetium, or thorium. The subsequent sections of this paper discuss calculations of the closed-shell electronic configurations for the conducting skeletons of each of the structures in Tables I and II. In all cases, the actual electronic configurations of the transition-metal–boron or metal–silicon subnetworks after receiving two electrons from each alkaline-earth atom and three electrons from each lanthanide atom are short of those required for the closed-shell structural unit, thereby providing holes in the valence band required for conductivity.

The dimensionality of the skeletal chemical bonding manifold[4] is related to the porosity of the region in the conducting skeleton where electron transport can occur. Globally delocalized skeletal bonding leads to a three-dimensional skeletal bonding manifold corresponding to dense delocalization of the conducting electrons or holes. Edge-localized skeletal bonding leads to a porous one-dimensional skeletal bonding manifold corresponding to only the 1-skeleton[10] of the polyhedral network,[4] thereby leading to porous delocalization of the conducting electrodes or holes. Such

(1) King, R. B.; Rouvray, D. H. *J. Am. Chem. Soc.* **1977**, *99*, 7834.
(2) King, R. B. In *Chemical Applications of Topology and Graph Theory*; King, R. B., Ed.; Elsevier: Amsterdam, 1983; pp 99-123.
(3) King, R. B. In *Molecules Structure and Energetics*; Liebman, J. F., Greenberg, A., Ed.; VCH Publishers: Deerfield Beach, FL, 1986; pp 123-148.
(4) King, R. B. *J. Math. Chem.* **1987**, *1*, 249.
(5) King, R. B. *Isr. J. Chem.*, in press.
(6) King, R. B. *J. Solid State Chem.* **1987**, *71*, 224.
(7) King, R. B. *J. Solid State Chem.* **1987**, *71*, 233.
(8) King, R. B. *Inorg. Chim. Acta* **1988**, *143*, 15.
(9) King, R. B. *J. Mater. Sci. Lett.* **1990**, *9*, 5.
(10) Grünbaum B. *Convex Polytopes*; Interscience: New York, 1967; p 138.

0020-1669/90/1329-2164$02.50/0

Table I. Superconducting Ternary Transition-Metal Boride Structures[a]

superconductor structure	T_c, K	closed-shell structural unit	electron deficiency per metal atom	transition-metal cluster units[b]	model molecular species[b]	lit. ref
$LuRh_4B_4$	11.5	$Rh_4B_4^{4-}$	0.25	Rh_4 tetrahedra (2.71)	$Rh_4(CO)_{12}$ (2.71)	7
$Ba_{0.67}Pt_3B_2$	5.6	$Pt_3B_2^{2-}$	0.22	Pt_3 triangles (2.65)	$[Pt_3(CO)_6]_n^{2-}$ (2.66)	13
$LuRuB_2$	10.0	RuB_2^{4-}	1.0	Ru_n chains (3.03)		15
$LuOs_3B_2$	4.5	$Os_3B_2^{6-}$	1.0	$Os_{6/4}$ trigonal prisms	$[Co_6(CO)_{15}C]^{2-}$	16

[a] For the ternary lanthanide transition-metal boride structures, the derivative with the highest T_c, namely the lutetium derivative, is listed in all cases. [b] Relevant metal–metal bond distances in Å are listed in parentheses.

Table II. Superconducting Ternary Transition-Metal Silicides

superconductor[a]	T_c, K	transition-metal network	Mt–Mt bond lengths, Å	structure	lit. ref
$Sc_5Ir_4Si_{10}$	8.4	isolated Ir	no Ir–Ir bonds	primitive tetragonal	28
$LaRu_3Si_2$	7.3	Kagomé net	2.76, 2.93	hexagonal	35
ThIrSi	6.5	isolated Ir	no Ir–Ir bonds	body-centered tetragonal	34
$Lu_2Fe_3Si_5$	6.0	Fe_∞ chains Fe_4 squares	2.64, 2.67	distorted $BaAl_4$ (primitive tetragonal)	26, 27
$La_2Rh_3Si_5$	4.4	Rh_∞ chains	2.8	$BaAl_4$ (orthorhombic)	25
LaPtSi	3.5	isolated Pt	no Pt–Pt bonds	body centered tetragonal (Like ThIrSi)	33
$LaRhSi_2$	3.4	isolated Rh	no Rh–Rh bonds		31
$LaRhSi_3$	2.3	isolated Rh	no Rh–Rh bonds	$BaAl_4$ (tetragonal)	23
$LaIr_2Si_2$	1.6	nets of squares	2.91	$BaAl_4$ (tetragonal)	29

[a] The derivative with a given structure having the highest T_c is listed. This derivative is generally one with a diamagnetic counterion such as Sc, La, or Lu.

porous delocalization appears to be characteristic of the superconducting structures discussed in this paper. The confinement of electron mobility to a porous conducting skeleton appears to facilitate the electron pairing required for superconductivity and may relate to a small BCS coherence length.[11]

Ternary Transition-Metal Borides

(A) $LnRh_4B_4$. These lanthanide rhodium borides are treated in detail in a previous paper.[7] Their structures consist of electronically linked Rh_4 tetrahedra in which each of the four triangular faces of each Rh_4 tetrahedron is capped by a boron atom of a B_2 unit (B–B distance of 1.86 Å in YRh_4B_4) leading to Rh_4B_4 cubes in which the edges correspond to 12 Rh–B bonds (average length of 2.17 Å in YRh_4B_4) and single diagonals in each face correspond to six Rh–Rh bonds (average length of 2.71 Å in YRh_4B_4). The ratio between these two lengths, namely 2.71/2.17 = 1.25 is only ~13% less than the $\sqrt{2}$ = 1.414 ratio of the lengths of a face diagonal to an edge in an ideal cube. The Rh–Rh distances of 2.71 Å in these Rh_4B_4 cubes are essentially identical with the mean Rh–Rh distance in the discrete molecular rhodium cluster $Rh_4(CO)_{12}$[12] regarded as a prototypical example of an edge-localized tetrahedron.[2,4]

The boron and rhodium atoms in $LnRh_4B_4$ have four and nine valence orbitals, respectively. All of these valence orbitals are used to form two-center bonds leading to an edge-localized structure. The four bonds formed by a boron atom include three internal bonds to rhodium atoms in the same Rh_4B_4 cube and one external bond to the nearest boron atom in an adjacent Rh_4B_4 cube leading to a discrete B_2 unit. The nine bonds formed by a rhodium atom include three internal bonds to the other rhodium atoms in the same Rh_4 tetrahedron, three internal bonds to boron atoms in the same Rh_4B_4 cube, and three external bonds to rhodium atoms in adjacent Rh_4B_4 cubes. Each boron atom and each rhodium atom thus use three and six internal orbitals, respectively, for the skeletal bonding and are therefore donors of 3 − 1 = 2 and 9 − 3 = 6 skeletal electrons, respectively, after allowing for the valence electrons required for external bonding. A neutral Rh_4B_4 cube in the $LnRh_4B_4$ structure thus has (4)(2) + (4)(6) = 32 skeletal electrons so that the $Rh_4B_4^{4-}$ tetraanion corresponds to the closed-shell electronic configuration with the 36 skeletal electrons required for an Rh_4B_4 cube with edge-localized bonds along each of the 12 edges (Rh–B bonds) and along a diagonal in each of the six faces (Rh–Rh bonds). Since the lanthanides also present in the lattice form tripositive rather than tetrapositive ions, the $LnRh_4B_4$ borides must be $Ln^{3+}Rh_4B_4^{3-}$ with the $Rh_4B_4^{3-}$ anion having one electron less than the closed-shell electronic configuration $Rh_4B_4^{4-}$. This electron deficiency of one electron per Rh_4 tetrahedron corresponds to the presence of holes in an otherwise filled valence band, thereby providing a mechanism for conductivity.

(B) $M^{II}_{0.67}Pt_3B_2$. The structures of these alkaline-earth platinum borides[13] consist of electronically linked Pt_3 triangles with each triangle capped above and below by boron atoms leading to Pt_3B_2 trigonal bipyramids with the three equatorial–equatorial edges corresponding to Pt–Pt bonds (average length of 2.65 Å in $Ba_{0.67}Pt_3B_2$) and the six axial-equatorial edges corresponding to Pt–B bonds (average length of 2.22 Å in $Ba_{0.67}Pt_3B_2$). The B–B distance of 2.29 Å is too long for a direct boron–boron two-center bond, but a pair of boron atoms separated by 2.29 Å can be regarded as the apices of a different flattened B_2Pt_3 trigonal bipyramid also with 2.22-Å Pt–B bonds as the six axial–equatorial edges but with the three Pt–Pt equatorial–equatorial edges too long for two-center chemical bonds. These B_2Pt_3 flattened trigonal bipyramids contain a five-center core bond with the required two electrons coming from the boron atoms. The infinite conducting skeleton in $M^{II}_{0.67}Pt_3B_2$ derivatives is essentially edge-localized, but unlike $LnRh_4B_4$, there are also pockets of delocalization in the $M^{II}_{0.67}Pt_3B_2$ structure (i.e., the five-center B_2Pt_3 core bonds in the flattened trigonal bipyramids), which may account for the generally lower T_c's of the $M^{II}_{0.67}Pt_3B_2$ derivatives relative to the $LnRh_4B_4$ derivatives. The Pt–Pt distances of 2.65 Å in the Pt_3 triangles in $Ba_{0.67}Pt_3B_2$ are very close to the Pt–Pt distances of 2.66 Å in the Pt_3 triangles in the stacked triangle platinum carbonyl cluster anions $[Pt_3(CO)_6]_n^{2-}$ (n = 2, 3, 5).[14]

This bonding model for the $M^{II}_{0.67}Pt_3B_2$ derivatives is consistent with simple electron and orbital bookkeeping, which suggests $Pt_3B_2^{2-}$ to be an edge-localized closed-shell structural unit with the deficiency of $^2/_3$ electron per Pt_3B_2 unit, accounting for the holes in the valence band required for conductivity. The nine valence orbitals on each platinum atom are used as follows:

(11) Fischer, Ø.; Decroux, M.; Chevrel, R.; Sergent, M. In *Superconductivity in d- and f-Band Metals*; Douglas, D. H., Ed.; Plenum Press: New York, 1976; pp 176–177.
(12) Carré, F.H.; Cotton, F. A.; Frenz, B. A. *Inorg. Chem.* **1976**, *15*, 380.
(13) Shelton, R. N. *J. Less-Common Met.* **1978**, *62*, 191.
(14) Calabrese, J. C.; Dahl, L. F.; Chini, P.; Longoni, G.; Martinengo, S. *J. Am. Chem. Soc.* **1974**, *96*, 2614.

2 internal orbitals for Pt–Pt equatorial–equatorial bonds within the Pt_3B_2 trigonal bipyramid
2 internal orbitals for Pt–B equatorial–axial bonds within the Pt_3B_2 trigonal bipyramid
2 external orbitals for Pt–Pt bonds (2.86 Å in $Ba_{0.67}Pt_3B_2$) to platinum atoms in Pt_3 triangles in adjacent edge-localized Pt_3B_2 trigonal bipyramids
1 empty external orbital for a five-center B_2Pt_3 core bond in an adjacent B_2Pt_3 flattened trigonal bipyramid
2 remaining nonbonding external orbitals each requiring lone electron pairs

Each platinum atom is a donor of four skeletal electrons as follows:

10 valence electrons from a neutral Pt atom	
−2 electrons for external Pt–Pt bonds	
−4 electrons for the two nonbonding external orbitals	
4 electrons remaining for skeletal electrons for the Pt_3B_2 edge-localized trigonal bipyramid	

Each boron atom is a donor of two skeletal electrons since one of its three valence electrons is needed for a B_2Pt_3 five-center bond in the core of the B_2Pt_3 flattened trigonal bipyramid. Since in $Pt_3B_2^{2-}$ each platinum vertex donates four skeletal electrons and each boron vertex donates two skeletal electrons, a $Pt_3B_2^{2-}$ unit has the (3)(4) + (2)(2) + 2 = 18 skeletal electrons required for two-center localized bonds along each of the nine edges of the $Pt_3B_2^{2-}$ trigonal bipyramid.

(C) $LnRuB_2$. The conducting skeleton of these lanthanide ruthenium borides consists of a chain of ruthenium atoms (Ru–Ru = 3.03 Å in $LuRuB_2$) in which each ruthenium atom is bonded to six boron atoms and each boron atom is bonded to three ruthenium atoms leading to $RuB_{6/3}$ structural units.[15] The boron atoms are tightly bonded in pairs (B–B = 1.74 Å in $LuRuB_2$) so that each boron atom has two of its three valence electrons available for bonding to ruthenium. The ruthenium atom in such a $RuB_2^{4-} = RuB_{6/3}^{4-}$ structural unit has the favored 18-electron rare gas configuration as follows:

neutral Ru atotm	8 electrons
2 Ru–Ru bonds to adjacent Ru atoms in the chain	2 electrons
$^6/_3$ boron atoms as ligands: (6/3)(2) =	4 electrons
−4 charge	4 electrons
electronic configuration of Ru atom in RuB_2^{4-}	18 electrons

Since the lanthanides in $LnRuB_2$, like those in $LnRh_4B_4$ discussed above, form tripositive rather than tetrapositive ions, the ruthenium atoms in $LnRuB_2$ have one valence electron less than the 18-electron closed-shell electronic configuration of RuB_2^{4-}. This electron deficiency corresponds to the presence of holes in an otherwise filled valence band, thereby providing a mechanism for conductivity. Furthermore, the conducting skeleton of $LnRuB_2$ consists solely of two-electron–two-center B–B, Ru–B, and Ru–Ru bonds, leading to the edge-localized type of conducting skeleton providing the porous delocalization associated with superconductivity.

(D) $LnOs_3B_2$. The lanthanide osmium borides $LnOs_3B_2$ and their ruthenium analogues[16] have structures analogous to those of $LnCo_3B_2$ constructed from boron-centered transition-metal trigonal prisms.[17] Each transition-metal atom is shared by four trigonal prisms, so that the fundamental structural unit of $LnOs_3B_2$ is the trigonal-prismatic cavity $Os_{6/4}B$. The bonding topology within a trigonal prismatic cavity is expected to be edge-localized like the discrete cobalt carbonyl carbide anion $[Co_6(CO)_{15}C]^{2-}$, which has a centered trigonal prismatic Co_6C unit.[18,19] In $LnOs_3B_2$, each of the nine edges of a single $Os_{6/4}B$ trigonal prism is shared between two such trigonal prisms so that a closed-shell electronic configuration for edge-localized bonding has (2)(9/2) = 9 skeletal electrons per trigonal prism corresponding to $Os_{6/4}B^{3-} = Os_3B_2^{6-}$ as follows:

6/4 Os vertices using 6 internal orbitals: (6/4)(2) =	3 electrons
1 boron atom in the center	3 electrons
−3 charge	3 electrons
total skeletal electrons per $Os_{6/4}B^{3-}$ trigonal prism	9 electrons

Note that 6 of the 8 valence electrons of a bare osmium vertex using 6 internal orbitals are required for the 3 external orbitals, thereby making such a vertex a donor of 2 skeletal electrons.

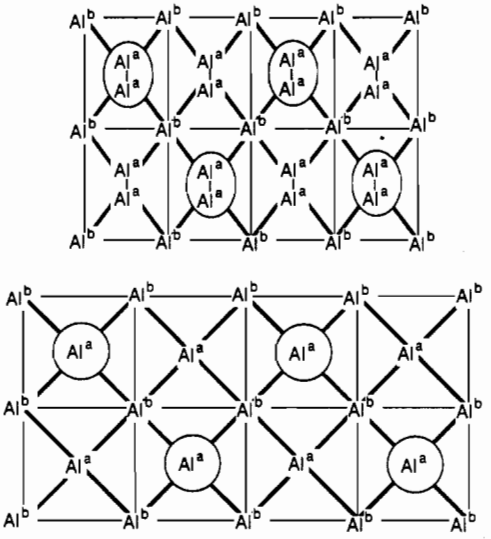

Figure 1. Two schematic views of the aluminum network in $BaAl_4$. Circled aluminum atoms inside the squares or rectangles appear in front of the page whereas uncircled aluminum atoms appear in back of the page.

Superconducting Ternary Transition-Metal Silicides with the $BaAl_4$ Structure

Table III summarizes the structural aspects of the four known types of superconducting ternary metal silicides with the $BaAl_4$ structure.[20,21] In these metal silicides, the transition metals (Mt) and silicon atoms occupy the aluminum sites and the lanthanides (Ln) occupy the barium sites in the $BaAl_4$ structure (Figure 1) thereby leading to (Mt + Si)/Ln ratios of 4 for all of these compound types. The transition-metal–silicon infinite network of tetragonal-pyramidal cavities in these structures may be regarded as the conducting skeleton. This conducting skeleton may either be edge-localized with eight skeletal electrons per tetragonal pyramidal cavity or delocalized with six skeletal electrons per tetragonal pyramidal cavity. The chemical bonding topology of such a delocalized tetragonal cavity is closely related to that in square-pyramidal *nido*-boranes such as B_5H_9.[22] The electronic configurations of each transition metal in the metal silicides in Table III arbitrarily assume edge-localized bonding as illustrated by the following calculation of the electronic configuration of the rhodium atom in the $RhSi_3^{3-}$ building block of $LaRhSi_3$[23] with the -3 charge arising from the La^{3+} counterion:

neutral Rh atom	9 electrons
1 apical silicon atom: (1)(4 − 4) =	0 electron
4/2 basal silicon atoms: (4/2)(4 − 2) =	4 electrons
−3 charge	3 electrons
total rhodium valence electrons:	16 electrons

In this case the apical silicon atom formally uses all of its four valence electrons as a hypervalent silicon atom similar to hypervalent RP vertices in (alkylphosphinidene)metal carbonyl clusters.[24] Each basal silicon atom uses two of its four valence

(15) Shelton, R. N.; Karcher, B. A.; Powell, D. R.; Jacobson, R. A.; Ku, H. C. *Mater. Res. Bull.* **1980**, *15*, 1445.
(16) Ku, H. C.; Meisner, G. P.; Acker, F.; Johnson, D. C. *Solid State Commun.* **1980**, *35*, 91.
(17) Niihara, K.; Yajima, S. *Bull. Chem. Soc. Jpn.* **1973**, *46*, 770.
(18) Martinengo, S.; Strumolo, D.; Chini, P.; Albano, V. G.; Braga, D. *J. Chem. Soc., Dalton Trans.* **1985**, 35.
(19) King, R. B. *New J. Chem.* **1988**, *12*, 493.
(20) Pearson, W. B. *J. Solid State Chem.* **1985**, *56*, 278.
(21) Zheng, C.; Hoffmann, R. *Z. Naturforsch.* **1986**, *41B*, 292.
(22) Muetterties, E. L., Ed. *Boron Hydride Chemistry*; Academic Press: New York, 1975.
(23) Lejay, P.; Higashi, I.; Chevalier, B.; Etourneau, J.; Hagenmuller, P. *Mater. Res. Bull.* **1984**, *19*, 115.

Table III. Superconducting Ternary Transition-Metal Silicides with the $BaAl_4$ Structure

superconductor	(Mt + Si) tetragonal pyramids[a] apical atoms	(Mt + Si) tetragonal pyramids[a] basal atoms	supplemental bonds per 8 (Mt + Si)[b]	tetragonal-pyramidal cavities	transition metals per cavity	transition-metal coordination sphere[c] apical	transition-metal coordination sphere[c] basal
$Lu_2Fe_3Si_5$	$(Fe(1))_2Si_2$	$(Fe(2))Si_3$	3 Fe–Fe (2.65) 3Fe–Si (2.30)	$Fe_{2/4}Si_{2/4}Si$ $Si_{4/4}Fe$	$^3/_4$	$(Fe(1))Si^a_{2/3}Si^b_{4/4}(Fe_2)$ ($16^1/_3$ electrons)	$(Fe(2))Si^a_{2/3}Si^b_{4/4}(Fe_2)$ ($15^1/_3$ electrons)
$La_2Rh_3Si_5$	$(Rh(1))_2Si_2$	$(Rh(2))Si_3$	1 Rh–Rh (2.8) 2 Rh–Si	$Rh_{2/4}Si_{2/4}Si$ $Si_{4/4}Rh$	$^3/_4$	$(Rh(1))Si^a_{1/3}Si^b_{2/3}Si^b_{2/4}$ (15 electrons)	$(Rh(2))Si^a_{4/3}Si^b_{2/3}(Rh_2)$ (17 electrons)
$LaRhSi_3$	Rh_2Si_2	Si_4	none	$Si_{4/4}Si$ $Si_{4/4}Rh$	$^1/_2$	$RhSi^aSi^b_{4/2}$ (16 electrons)	
$LaIr_2Si_2$ (LT)[d]	Si_4	Ir_4	8 Ir–Ir (2.90)	$Ir_{4/4}Si$	1		$IrSi_{4/4}(Ir_4)$ ($17^1/_2$ electrons)
$LaIr_2Si_2$ (HT)[d]	$(Ir(1))_2Si_2$	$(Ir(2))_2Si_2$	4 Ir–Ir (2.96)	$Si_{4/4}Ir$	1	$(Ir(1))Si^a_{1/5}Si^b_{4/4}$ ($15^3/_{10}$ electrons)	$(Ir(2))Si^a_{4/5}(Ir_4)$ ($17^3/_{10}$ electrons)

[a] The numbering of the transition-metal atoms is the same as that given in the literature. [b] The bond distances in Å are given in parentheses. [c] Si^a = apical silicon; Si^b = basal silicon; direct transition-metal–metal bonds in the coordination sphere are given in parentheses; electron counts assume edge-localized bonding. [d] LT = low temperature form; HT = high temperature form; see: Braun, H. F.; Engel, N.; Parthe, E. *Phys. Rev.* **1983**, *B28*, 1389.

electrons for two-electron–two-center bonds in the two assumed edge-localized rhodium-free $Si_{4/4}Si$ tetragonal pyramidal cavities of which it is a vertex. This leaves 4 – 4 = 0 valence electron and 4 – 2 = 2 valence electrons for the apical and basal silicon atoms, respectively, for the $Si_{4/4}Rh$ cavity. The observed transition-metal valence electron configurations clustering around 16 electrons rather than the usual 18 electron rare gas configurations can be an artifact of assuming edge-localized rather than delocalized bonding in the tetragonal-pyramid cavities since as noted above a delocalized tetragonal-pyramid cavity requires two skeletal electrons less than an edge-localized tetragonal-pyramid cavity leaving two more electrons for a transition metal associated with the cavity.

An important aspect of the bonding in most superconducting ternary transition-metal silicides based on the $BaAl_4$ structure is the presence of supplemental bonding in the conducting skeleton. Figure 2 shows the two schematic views of the $Rh_3Si_5^{6-}$ conducting skeleton in the $La_2Rh_3Si_5$ structure[25] analogous to the corresponding views of the Al_4^{2-} skeleton in $BaAl_4$. Each basal rhodium forms four supplemental bonds for a coordination number of 8 within the $Rh_3Si_5^{6-}$ conducting skeleton. Two of these supplemental bonds are to adjacent basal rhodium atoms (heavy lines in Figure 2 (bottom)), and the other two of these supplemental bonds are to adjacent basal silicon atoms, leading to the distortion of the square lattice of the bases of the fused tetragonal pyramids in the directions indicated by arrows in Figure 2 (bottom). Thus all of the edges of the lattice of tetragonal pyramid bases with a rhodium atom at one or both ends represent two-electron–two-center bonds. The rhodium–rhodium bonding subnetwork consists of infinite chains of bonded basal rhodium atoms. The apical rhodium atoms in $La_2Rh_3Si_5$ form only the five Rh–Si bonds required by their positions in the $BaAl_4$ structure (Table I) and thus participate in neither the rhodium–rhodium bonding subnetwork nor the supplemental edge-localizing bonding. Superimposition of the network of edge-localized supplemental bonding onto a possibly delocalized conducting skeleton of fused tetragonal pyramids provides a conducting pathway similar to the porously delocalized conducting skeleton in Chevrel phases[6] and ternary metal borides.[7]

A more complicated and extensive supplemental bonding network is found in the 6.0 K superconductor $Lu_2Fe_3Si_5$[26,27] as depicted schematically in Figure 3. In this case, the supplemental bonding involves the apical atoms as well as the basal atoms of the $Fe_3Si_5^{6-}$ conducting skeleton, leading to more extensive distortion of the fundamental $BaAl_4$ structure (Figure 1). Furthermore, the $Fe_3Si_5^{6-}$ conducting skeleton is constructed from alternating layers of basal planes of two types (Figure 3 (bottom, left and right)), which with the associated apical atoms have

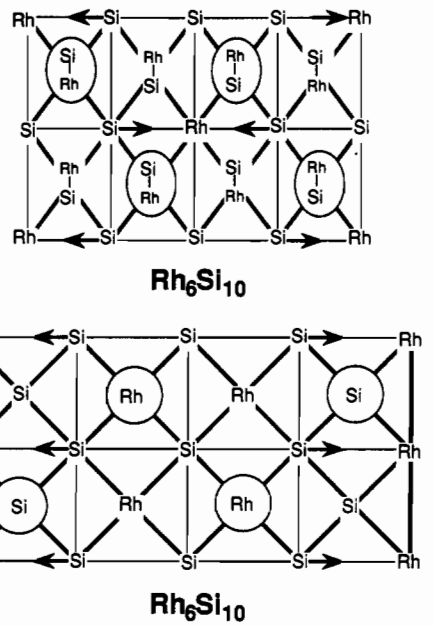

Figure 2. Two schematic view of the Rh_6Si_{10} conducting skeleton in $La_2Rh_3Si_5$. Circled atoms inside the squares or rectangles appear in front of the page whereas uncircled atoms appear in back of the page. Heavy lines in the bottom view correspond to direct Rh–Rh bonds (2.8 Å) whereas arrows correspond to distortions of basal silicon atoms to form direct Rh–Si bonds.

stoichiometries Si_2Fe_2 and Si_3Fe leading to the observed overall stoichiometry $Si_2Fe_2 + Si_3Fe = Si_5Fe_3$. The iron–iron bonding subnetwork consists of both infinite chains of bonded basal iron atoms and isolated squares of bonded apical iron atoms (Figure 3) using one-third and two-thirds of the iron atoms, respectively.

Other Superconducting Ternary Metal Silicides

The superconducting ternary lanthanide transition-metal silicides other than those based on the $BaAl_4$ structure discussed above, can be considered to have edge-localized transition-metal–silicon conducting skeletons with lanthanide counterions. The apparent electronic configuration of the transition metals will be slightly less than the closed-shell electronic configuration (typically the 18-electron rare gas configuration except for $LaRu_3Si_2$), indicative of holes in the valence band required for conductivity similar to that of the ternary lanthanide transition-metal borides. Details of specific structure types are outlined below. These details also illustrate electron-counting procedures for ternary metal silicides, including those discussed above based on the $BaAl_4$ structure.

(A) $Sc_5Ir_4Si_{10}$.[28] This superconductor has a T_c of 8.4 K, which is the highest of any of the ternary transition-metal silicide su-

(24) King, R. B. *New J. Chem.* **1989**, *13*, 293.
(25) Chevalier, B.; Lejay, P.; Etourneau, J.; Vlasse, M.; Hagenmuller, P. *Mater. Res. Bull.* **1982**, *17*, 1211.
(26) Bodak, O. I.; Kotur, B. Ya.; Yarovets, V. I.; Gladyshevskii, E. I. *Sov. Ppys. Crystallogr.* **1977**, *22*, 217.
(27) Braum, H. F. *Phys. Lett.* **1980**, *75A*, 386.
(28) Braun, H. F.; Segre, C. U. *Solid State Commun.* **1980**, *35*, 735.

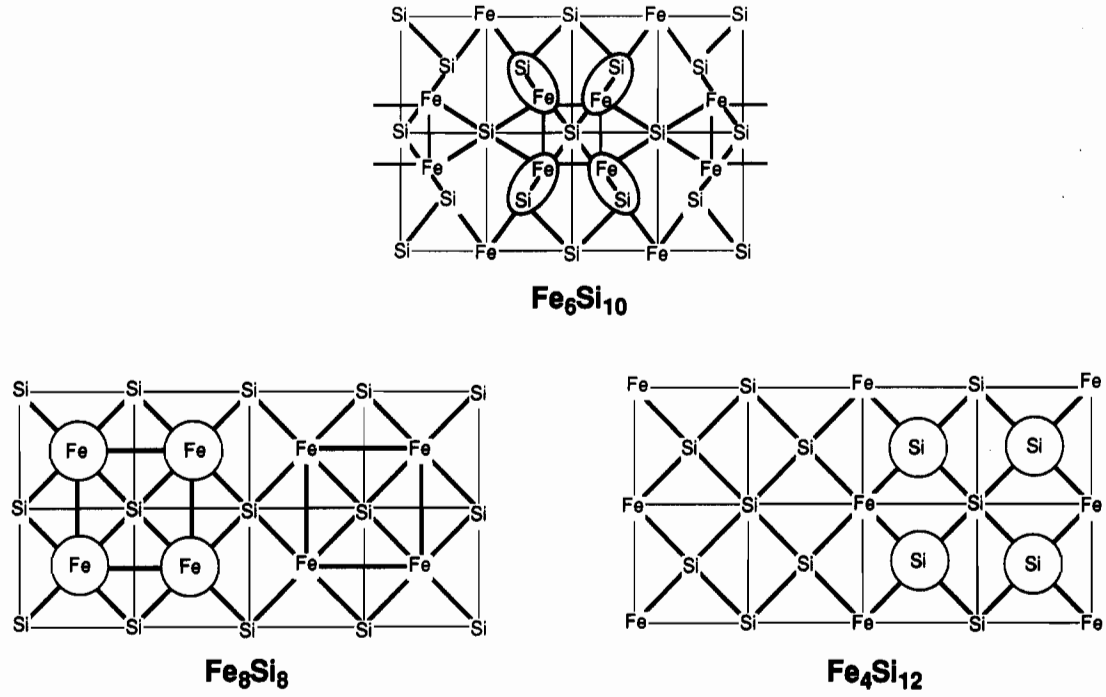

Figure 3. Two schematic views of the $Fe_6Si_{10} = {}^1/_2(Fe_8Si_8 + Fe_4Si_{12})$ conducting skeleton in $Lu_2Fe_3Si_5$. Circled atoms inside the squares or rectangles appear in front of the page whereas uncircled atoms appear in back of the page. Direct Fe–Fe bonds (2.64 and 2.67 Å) are shown by heavy lines.

perconductors.[29] The structure of $Sc_5Ir_4Si_{10}$ is the same as that of its cobalt analogue, $Sc_5Co_4Si_{10}$, which has been studied in some detail.[30] In the $Sc_5Co_4Si_{10}$ structure, all cobalt atoms are equivalent and there are no cobalt–cobalt bonds. There are the following three types of silicon atoms with the indicated bonding within the cobalt–silicon conducting skeleton: (a) Si(1) bonded to 2 Co and 1 Si(1); (b) Si(2) bonded to 2 Co and 1 Si(2); (c) Si(3) bonded to 2 Co. Si(1) and Si(2) are considered to be planar and thus donate three electrons to two cobalt atoms after allowing one of the four valence electrons for a Si–Si bond. Si(3) is considered to be bent with two lone electron pairs like the oxygen atom in water and thus cannot formally donate electrons to cobalt. Each cobalt atom is bonded to five silicon atoms (1 Si(1) + 2 Si(2) + 2 Si(3)) leading to $Co(Si(1))_{1/2}(Si(2))_{2/2}(Si(3))_{2/2}$ structural units having an average charge of $-(3)(5)/4 = -3^3/_4$ to neutralize the Sc^{3+} counterions. This leads to $17^1/_4$ average valence electrons for each cobalt atom as follows:

neutral Co atom	9 electrons
1/2 Si(1): (1/2)(3) =	$1^1/_2$ electrons
2/2 Si(2): (2/2)(3) =	3 electrons
2/2 Si(3): (2/2)(0) =	0 electron
$-3^3/_4$ charge	$3^3/_4$ electrons
average cobalt valence electrons:	$17^1/_4$ electrons

Since cobalt is in the same column of the periodic table as iridium, the average valence electron configuration of the iridium atoms in the isostructural $Sc_5Ir_4Si_{10}$ is also $17^1/_4$.

(B) $LaRhSi_2$.[31] The 3.4 K superconductor $LaRhSi_2$ has the $CeNiSi_2$ structure,[32] which has no direct transition-metal–metal bonds. The silicon atoms are of two types: (a) Si(1) bonded to 2 other Si(1) and 1 Rh in a trigonal-planar coordination within the rhodium–silicon conducting skeleton leading to bonded zigzag chains of Si(1) atoms; (b) Si(2) bonded to 4 Rh. Each rhodium atom is bonded to five silicon atoms (1 Si(1) + 4 Si(2)) leading to $Rh(Si(1))(Si(2))_{4/4}$ structural units with an average charge of −3 to neutralize the La^{3+} counterions. This leads to 18 average valence electrons for each rhodium atom as follows:

neutral Rh atom	9 electrons
Si(1): (1)(4–2) =	2 electrons
Si(2): (4/4)(4) =	4 electrons
−3 charge	3 electrons
average rhodium valence electrons	18 electrons

Even though the rhodium atoms thus have the closed-shell 18-electron rare-gas configuration, the empty p orbital implied by the planar configuration of Si(1) within the rhodium–silicon conducting skeleton used to calculate this 18-electron rhodium configuration can correspond to holes in the valence band required for conductivity in this infinite structure.

(C) LaPtSi[33] and ThIrSi.[34] These isostructural superconductors have structures with neither transition-metal–metal nor silicon–silicon bonds. Each transition metal is bonded to three silicon atoms, and each silicon atom is bonded to three transition-metal atoms, leading to the building blocks $PtSi_{3/3}^{3-}$ and $IrSi_{3/3}^{4-}$ for LaPtSi and ThIrSi, respectively, with the indicated negative charges neutralizing the La^{3+} and Th^{4+} counterions, respectively. This leads to 17 average valence electrons for each transition metal atom as illustrated below for the $PtSi_{3/3}^{3-}$ building block in LaPtSi:

neutral Pt atom	10 electrons
3/3 Si atom: (3/3)(4) =	4 electrons
−3 charge	3 electrons
average platinum valence electrons	17 electrons

(D) $LaRu_3Si_2$.[35] This superconductor structure is different from all of the other ternary transition-metal silicides discussed in this paper in being "metal rich" with more transition metal (ruthenium) atoms than silicon atoms. Nevertheless, an edge-localized model can be used for the $RuSi_{4/6}^-$ conducting skeleton of this structure, which has only one type of ruthenium atom and only one type of silicon atom. Each ruthenium atom is bonded to four silicon atoms in a nearly planar arrangement as well as to four other ruthenium atoms (2 Ru–Ru = 2.76 Å and 2 Ru–Ru = 2.93 Å)

(29) Braun, H. F. *J. Less-Common Met.* **1984**, *100*, 105.
(30) Braun, H. R.; Yvon, K.; Braun, R. M. *Acta Crystallogr.* **1980**, *B36*, 2397.
(31) Chevalier, B.; Lejay, P.; Etourneau, J.; Hagenmuller, *Mater. Res. Bull.* **1983**, *18*, 315.
(32) Bodak, O. P.; Gladyshevskii, E. I. *Sov. Phys. Crystallogr.* **1970**, *14*, 859.
(33) Evers, J.; Oehlinger, G.; Weiss, A.; Probst, C. *Solid State Commun.* **1984**, *50*, 61.
(34) Lejay, P.; Chevalier, B.; Etourneau, J.; Tarascon, J. M.; Hagenmuller, P. *Mater. Res. Bull.* **1983**, *18*, 67.
(35) Vandenberg, J. M.; Barz, H. *Mater. Res. Bull.* **1980**, *15*, 1493.

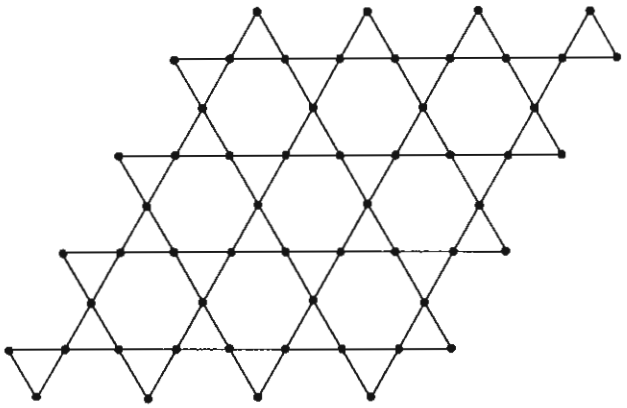

Figure 4. Triangular Kagomé net of bonded ruthenium atoms in $LaRu_3Si_2$.

leading to a Kagomé triangular lattice (Figure 4) of bonded ruthenium atoms. Each silicon atom is in the center of an Ru_6 trigonal prism and is therefore bonded to six ruthenium atoms. There are no silicon–silicon bonds. The edges of the triangular faces ("horizontal" edges) of the trigonal prism correspond to bonding Ru–Ru distances (2.76 and 2.93 Å as indicated above) but the edges of only rectangular faces ("vertical" edges) of the trigonal prism correspond to nonbonding Ru···Ru distances (3.57 Å). The ruthenium atoms in the $RuSi_{4/6}^-$ building block of the conducting skeleton of $LaRu_3Si_2$ have $15^2/_3$ average valence electrons as follows:

neutral Ru atom	8 electrons
4 Ru–Ru bonds:	4 electrons
4/6 Si atom: (4/6)(4) =	$2^2/_3$ electrons
−1 charge:	1 electron
average ruthenium electronic configuration	$15^2/_3$ electrons

This $15^2/_3$ electron average configuration of the ruthenium atoms may be considered to be $^1/_3$ electron short of the 16 electrons required for the two-dimensional toroidal bonding manifold[36] found for a square-planar late transition metal such as the d^8 metals Rh(I), Ir(I), Pd(II), Pt(II), and Au(III) and consistent with the observed[35] planar coordination of four silicon atoms around a central ruthenium atom in the $LaRu_3Si_2$ structure.

A-15 Alloys

Before the discovery of the high T_c copper oxide superconductors, the highest T_c's were found in alloys having the A-15 structure and the stoichiometry M_3E where M is Nb or V and E is Ga, Si, Ge, or Sn.[37,38] The methods outlined in this paper suggest a model for the skeletal bonding topology exhibiting the porous delocalization associated with superconductivity.

Consider V_3Si as the prototypical A-15 alloy, which may be regarded as isoelectronic with the important A-15 superconductors Nb_3Ge and Nb_3Sn. Figure 5 depicts a cubic building block $V_{12/2}SiSi_{8/8} = V_6Si_2$ of the A-15 structure in which the silicon and vanadium atoms are represented by shaded and open circles, respectively. This structure has the following features. (A) A silicon atom is in the center of the cube (=Si). (B) Silicon atoms are at the eight vertices of the cube, which are each shared with seven other cubes ($=Si_{8/8}$). (C) Pairs of vanadium atoms are in each of the six faces of the cube. Each pair is shared with the adjacent cube sharing the same face ($=V_{12/2}$). (D) The vanadium pairs in the six faces are oriented to form infinite straight vanadium chains in each of the three orthogonal directions. These chains are depicted schematically in Figure 6 where for clarity each infinite straight vanadium chain is depicted as a straight tube. These chains comprise the essential portion of the conducting skeleton. (E) The polyhedron formed by the 12 vanadium atoms around the central silicon atom is topologically an icosahedron

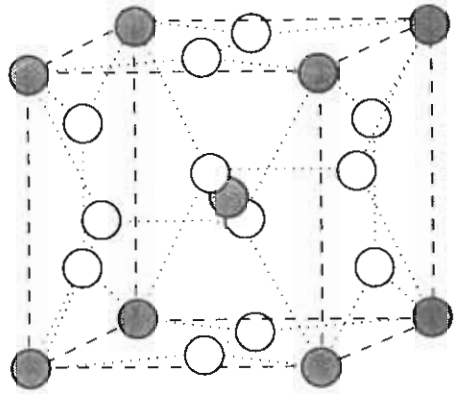

Figure 5. V_6Si_2 cubic building block for V_3Si and related A-15 superconductors. Shaded circles in the center and at each of the eight vertices correspond to silicon atoms whereas the pairs of open circles in each of the six faces correspond to vanadium atoms.

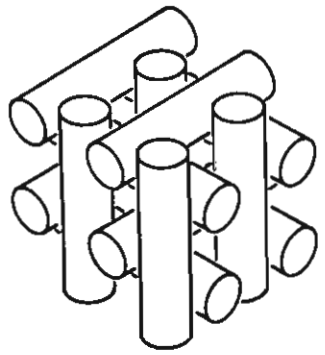

Figure 6. Infinite straight vanadium chains in each of the three orthogonal directions in the A-15 structure of V_3Si. Vanadium chains are depicted as straight tubes suppressing for clarity indications of individual vanadium atoms and the two-center V–V bonds.

with twenty triangular faces, eight of which are capped by the vertex silicon atoms forming tetrahedral V_3Si cavities. The 12 uncapped faces of the V_{12} icosahedron occur in six "diamond pairs" of the following type:

Consider a chemical bonding topology for V_3Si in which there are two-electron–two-center V–V bonds in the infinite straight vanadium chains in the three directions (Figure 6). Six such vanadium chains touch a given V_6Si_2 reference cube (Figure 5), namely one in each face. The V–V bonds of the vanadium chains, although equivalent in the overall structure, are of the following two types relative to a V_6Si_2 reference cube with which they are associated: (A) The first type consists of bonds between two vanadium atoms in a given face of the V_6Si_2 reference cube. Such V–V bonds are shared only between the two cubes sharing the face containing the vanadium atoms. (B) The second type consists of bonds between a vanadium atom and the adjacent vanadium atom in the chain *not* associated with the V_6Si_2 reference cube. Such V–V bonds are shared between four adjacent V_6Si_2 cubes. A given V_6Si_2 cube has six V–V bonds of type A and 12 V–V bonds of type B. Thus the V–V bonds associated with a given V_6Si_2 reference cube require (2)(6/2 + 12/4) = 12 skeletal electrons and use an equivalent number of vanadium valence orbitals since two-center–two-electron bonds are being considered.

The chemical bonding topology for V_3Si summarized in Table IV can now be defined relative to a V_6Si_2 reference cube. Since each vanadium atom uses nine valence orbitals ($=sp^3d^5$) and each silicon atom uses four valence orbitals ($=sp^3$), the 54 vanadium orbitals and eight silicon orbitals required for the bonding topology in Table I correspond to exactly what is available in a V_6Si_2 cube. A neutral V_6Si_2 cube has (6)(5) + (2)(4) = 38 valence electrons, which is two less than the 40 valence electrons required for the

(36) King, R. B. *Inorg. Chim. Acta* **1986**, *116*, 109.
(37) Leger, J. M. *J. Low Temp. Phys.* **1974**, *14*, 297.
(38) Johnson, G. R.; Douglass, D. H. *J. Low. Temp. Phys.* **1974**, *14*, 575.

Table IV. Chemical Bonding Topology of V_3Si and Related A-15 Superconductors Such As Nb_3Ge and Nb_3Sn

bond type	per V_6Si_2 cube: no. of such bonds	no. of electrons required	no. of V orbitals required	no. of Si orbitals required
2-center V–V bonds in chains (Figure 2)	6	12	12	0
4-center V_3Si bonds in V_3Si tetrahedral cavities	8	16	24	8
3-center V_3 bonds in one V_3 face of each diamond pair	6	12	18	0
tot. electrons and orbitals required for one V_6Si_2 cube		40	54	8

chemical bonding topology outlined in Table IV, implying that $V_6Si_2^{2-}$ is the closed-shell electronic configuration for this chemical bonding topology. This model for the chemical bonding in the A-15 superconductors V_3Si and its analogues Nb_3Ge and Nb_3Sn thus has the following features associated with superconductivity: (A) a porous conducting skeleton of which straight chains of V–V edge-localized bonds (Figure 6) are an important component; (B) holes in the valence band since $V_6Si_2^{2-}$ rather than V_6Si_2 is the closed-shell electronic configuration.

Superconductivity and Metal Valence Electrons

The structures of bulk metals may be constructed from building blocks of metal octahedra. The chemical bonding within a single isolated metal octahedron is most commonly globally delocalized with a single six-center core bond (e.g., $Rh_6(CO)_{16}$) although examples of face-localized metal octahedra with three-center bonds in each of the eight faces (e.g., $Nb_6X_{12}L_6^{2+}$) and edge-localized metal octahedra with two-center bonds along each of the 12 edges (e.g., $Mo_6X_8L_6^{4+}$) are also known.[39] Infinite fusion of metal octahedra in one, two, and three dimensions leads to metal cluster chains (e.g., Gd_2Cl_3), metal cluster sheets (e.g., ZrCl), and bulk metals, respectively. The skeletal electron and orbital counts in the infinite one-dimensional chains of the Gd_2Cl_3 type and the infinite two-dimensional sheets of the ZrCl type suggest six-center core bonds in each octahedral cavity and multicenter bonds in the two tetrahedral cavities for each octahedral cavity.[39] Such an electron and orbital analysis can be extended to bulk metals as infinite arrays of fused octahedra in all three dimensions with two tetrahedral cavities for each octahedral cavity. Since each metal atom in such bulk metals is shared by six octahedral cavities and since an octahedral cavity is formed by six metal atoms, the number of valence electrons for each octahedral cavity is equal to the number of valence electrons of the metal. Formation of one multicenter bond each in each octahedral cavity and in the two tetrahedral cavities for each octahedral cavity requires six electrons per octahedral cavity corresponding to a group 6 metal atom with six valence electrons such as chromium, molybdenum, or tungsten. Such a bonding topology for these metals is fully dense and is very unfavorable for the mobile electron pairs required for superconductivity in accord with the very low T_c's (<0.1 K) observed for pure chromium, molybdenum, and tungsten.[40,41] The "pseudo-closed-shell" electron configurations for chromium, molybdenum, and tungsten can also be related to other physical properties of these metals, including heats of atomization[42] and properties connected with the "transition-metal divide" of Stone.[43]

Now consider the group 5 metals vanadium, niobium, and tantalum, which have much higher T_c's than the group 6 metals considered above. The above bonding model leaves only a single electron rather than an electron pair for one of the three multicenter bonds associated with a given octahedral cavity (including two tetrahedral cavities for a given octahedral cavity). These single electrons can interact to form the Cooper pairs required for superconductivity accounting for the much higher T_c's of group 5 metals relative to the group 6 metals and the local maximum in the T_c versus Z_{av} curve at $Z_{av} = 4.8$ for transition-metal alloys.[40,41] Similarly, for the group 7 metals technetium and rhenium, the above bonding model leaves an extra electron after providing electron pairs for each of the three multicenter bonds associated with a given octahedral cavity. Pairing of these extra electrons can lead to the Cooper pairs required for superconductivity thereby accounting for the much higher T_c's of group 7 metals relative to the group 6 metals and the local maximum in the T_c versus Z_{av} curve at $Z_{av} = 7$ for transition-metal alloys. The smaller local maximum in the T_c versus Z_{av} curve at $Z_{av} = 3.3$ may have a similar origin based on pairing of the single electron remaining from each metal atom after an electron pair is provided for each six-center core bond in the centes of the octahedral cavities with no multicenter bonds in the tetrahedral cavities.

Acknowledgment. I am indebted to the Office of Naval Research for partial support of this work.

(39) King, R. B. *Inorg. Chim. Acta* **1987**, *129*, 91.
(40) Matthias, B. T. *Phys. Rev.* **1955**, *97*, 74.
(41) Matthias, B. T. In *Progress in Low Temperature Physics II*; Gorter, C. J., Ed.; North Holland: Amsterdam, 1975; Chapter 5, pp 138–150.
(42) Dasent, W. E. *Inorganic Energetics*; Penguin: Baltimore, MD, 1970.
(43) Stone, H. E. N. *Acta Metall.* **1979**, *27*, 259.

Notes

Contribution from the Chemistry Department, Rutgers, The State University of New Jersey, New Brunswick, New Jersey 08903

Spin Crossover and Light-Induced Excited-Spin-State Trapping in Bis(thiocyanato)bis(2,2′-bi-2-thiazoline)iron(II) and Bis(selenocyanato)bis(2,2′-bi-2-thiazoline)iron(II)

D. C. Figg and R. H. Herber*

Received July 25, 1989

The iron(II) complexes $Fe(bt)_2(NCS)_2$ (I) and $Fe(bt)_2(NCSe)_2$ (II), where bt = 2,2′-bi-2-thiazoline, have been shown to undergo a thermally driven high-spin (HS, $S = 2$) to low-spin (LS, $S = 0$) transition in the solid state.[1] Several techniques, including ^{57}Fe Mössbauer spectroscopy, powder X-ray diffraction,[2] magnetic susceptibility,[1,3] calorimetry,[4] single-crystal X-ray diffraction, and EPR spectroscopy,[5] have been utilized to study the spin-crossover transition of the isothiocyanate complex in some detail. The spin-crossover transition of the isoselenocyanate complex has been studied by using magnetic susceptibility,[1] ^{57}Fe Mössbauer spec-

(1) Bradley, G.; McKee, V.; Nelson, S. M.; Nelson, J. *J. Chem. Soc., Dalton Trans.* **1978**, 522.
(2) König, E.; Ritter, G.; Irler, W.; Nelson, S. M. *Inorg. Chim. Acta* **1979**, *37*, 169.
(3) Müller, E. W.; Spiering, H.; Gütlich, P. *J. Chem. Phys.* **1983**, *79*, 1439.
(4) Kulshreshtha, S. K.; Sasikala, R.; König, E. *Chem. Phys. Lett.* **1986**, *123*, 215.
(5) Ozarowski, A.; McGarvey, B. R.; Sarkar, A. B.; Drake, J. E. *Inorg. Chem.* **1988**, *27*, 628.

0020-1669/90/1329-2170$02.50/0